

**The Effect of Iron Oxide on Dissimilatory Nitrate Reduction to Ammonium
(DNRA) in Lignin Cellulose medium**

Megan Carpenter¹

Mentors: Joe Vallino² and Anne Giblin²

1. Lafayette College, 111Quad Drive, Easton, PA
2. The Ecosystems Center, MBL, Woods Hole, MA 02543

Abstract

The fate of nitrate in polluted groundwater entering a permeable reactive barrier (PRB) is uncertain. The major pathway of nitrate removal in this system is thought to be denitrification, but DNRA pathways leading to the production of ammonium are also likely. One DNRA pathway is carried out by chemolithoautotrophs that couple the reduction of nitrate with the oxidation of reduced sulfur forms. Ammonium is a biologically available form of nitrogen that may be more harmful than nitrate. In order to reduce ammonium production I proposed to add iron oxide to miniature PRBs in the laboratory to capture hydrogen sulfide (H₂S) because it is necessary for sulfur oxidizing bacteria capable of DNRA. It was concluded that the iron addition actually prevented the reduction of sulfate to H₂S because Fe (III) reducers outcompete sulfate reducers for electron donors. The iron addition did not affect nitrate removal and decreased the amount of ammonium production.

Introduction

Increased human population and urbanization of coastal areas has resulted in the release of large quantities of anthropogenic nitrogen into coastal habitats. Sources of nitrogen loading include agricultural and home fertilizers, septic tank waste, and atmospheric deposition in the form of nitrate. This nutrient pollution or eutrophication in coastal systems has been considered a major threat to the health of marine ecosystems for more than 30 years (Andersen, 2006).

Studies completed in Waquoit Bay, located off the western shore of Cape Cod, Mass., indicate that nitrogen loading rates are directly related to macroalgal populations (Valiela, 1995). The algae can kill native eelgrass by shading it and sometimes uprooting it. Eelgrass beds provide a home for snails, bryozoans, worms, young Bay scallops, herring, flounder and are also a food source for more mobile organisms (Schwarzman, 2002). The decomposition of large populations of algae can deplete the water column of oxygen which may lead to fish and shellfish death (Schwarzman, 2002). This over population of macroalgae, extensive loss of eelgrass and its corresponding inhabitants are results of eutrophication.

A low cost and maintenance solution to this problem may be the installation of a permeable reactive barrier (PRB), which is installed to intercept high nitrogen groundwater before reaching estuaries. A PRB contains a mixture of woodchips, limestone, sand, and gravel which provide a high carbon environment to facilitate denitrification and eliminate nitrate before it reaches coastal waters. Although denitrification is thought to be the main nitrate pathway, it is still unclear how the nitrate is removed.

In addition to the denitrification pathway, the nitrate can be converted into ammonium via dissimilatory nitrate reduction to ammonium (DNRA). Ammonium is a more bioavailable and less mobile form of nitrogen and can have more significant impacts in the environment. One form of DNRA couples the reduction of nitrate with the oxidation of reduced sulfur forms (Burgin, 2006). Concentrations of free sulfide are known to inhibit the final two reduction steps in the denitrification pathway, leading to the production of ammonium via DNRA

instead of N_2 gas (Burgin, 2006). Another DNRA pathway uses fermentation reactions to couple electron flow from organic matter to the reduction of nitrate. This process is thought to be favored in a low nitrate, high carbon environment (Burgin, 2006).

The PRB located at the head of Waquoit Bay experiences sea water intrusion and was shown to have sulfate concentrations around 5-6 mM. The same PRB also showed higher ammonium concentrations, reaching 30 μ M leaving the barrier (Vincent, 2006). This ammonium can be a result of remineralization of bacterial biomass, or DNRA. In the anaerobic conditions present in the PRB, it is likely that the sulfate is being reduced to hydrogen sulfide and becoming available to sulfur oxidizing bacteria capable of DNRA.

In order to reduce and possibly eliminate the production of ammonium in the permeable reactive barriers, I propose to use microcosms that simulate the conditions of the PRB located at Waquoit Bay. Iron oxide will be added to the wood chips in an effort to minimize ammonium production. Iron will essentially capture the hydrogen sulfide produced in anoxic parts of the microcosm by reacting with it and forming FeS. The iron will eliminate hydrogen sulfide which is (1) necessary for sulfur oxidizing bacteria with DNRA capability and (2) inhibitory to the final two steps of denitrification.

Methods

Assembling Microcosms

Four microcosms were assembled to simulate sea water entering and leaving the PRB located at Waquoit Bay. Each microcosm was made of 10 cm diameter PVC pipes, approximately 60 cm in depth. The microcosms were filled with woodchips and topped off with a layer of sand 5 cm from the top of the PVC pipe. A mesh lining was placed between the sand and woodchips to maintain separation. Filtered sea water spiked with 200 μ M nitrate dripped from a Marriot bottle apparatus located above the microcosms at a rate of 2.5 L d^{-1} into the system. The water flowed through the microcosm at a rate of 28 cm d^{-1} . Each column has an outflow tube located at the bottom of the microcosms in order to take samples. The water leaving the microcosms was released into a 1 liter graduated cylinder that is the same height as the top of the microcosm in order to keep the wood chips submerged in water and create an anaerobic environment. The 1 L graduated cylinder was placed in a bucket to allow for overflow. Two microcosms contained wood chips treated with iron oxide and two microcosms contained control woodchips.

Miniature wells were inserted at 2, 4, 8, 16, and 32 cm in one iron and one control microcosm in order to take samples at depths within the miniature PRBs.

The iron oxide substance was made by dissolving 500 grams of $FeCl_3$ in 2 liters of water containing 3 ml of 5 N HCl. In order to raise the pH of this solution to \sim 8, 500 mL of a 40 g/L solution of sodium hydroxide (NaOH) was added. The solution began to precipitate out and resulted in sludge like iron oxide. The iron oxide was homogenized with wood chips from two microcosms and exposed to air for 48 hours before adding them to the microcosms.

Sampling

Original woodchips and control and iron treated woodchips that composed the microcosms were analyzed for iron content.

After the spiked filtered sea water ran through the microcosms containing woodchips for approximately one week, conditions in the microcosm stabilized. The inflow and outflow water was filtered using 25 mm GF/F filters. Inflow water was analyzed for nitrate (NO_3), ammonium (NH_4), and sulfate (SO_4^{-2}). Outflow water was analyzed for nitrate (NO_3), ammonium (NH_4), sulfate (SO_4^{-2}), hydrogen sulfide (H_2S), and iron (Fe). Inflow water samples were taken each time the inflow water was replaced and outflow water samples were taken every 2-3 days. Samples were taken from 2, 4, 8, 16, and 32 cm at the end of experiment in one iron and one control microcosm. Each depth was analyzed for nitrate (NO_3), ammonium (NH_4), sulfate (SO_4^{-2}), and hydrogen sulfide (H_2S). Approximately 20 mL of sample was taken for nitrate, ammonium, sulfate, and iron analysis, and approximately 5 mL of sample was taken for hydrogen sulfide analysis and placed in scintillation vials.

Original woodchips and woodchips from 8 and 32 cm in each microcosm were analyzed for carbon and nitrogen analysis.

Techniques used for analysis

Nitrate samples were frozen until further analysis and ammonium samples were refrigerated and preserved using 10 μL of 5 N HCl. Sulfate samples were bubbled for 10 minutes using nitrogen gas and refrigerated. Approximately 250 μL of sample was added to 6 mL of 2% zinc acetate and stored in the refrigerator for sulfide analysis. Iron samples were acidified with 50 μL 5 N HCl and refrigerated.

Analysis

In order to determine nitrate concentrations, the samples were thawed and analyzed with the Lachat Flow Injection Analyzer (FIA) using a method adapted from Wood et.al.

The ammonium analysis technique is a modification of the phenol-hypochlorite method (Solarzano, 1969). Standards were made using a 10,000 μM ammonium chloride stock solution at concentrations of 0, 0.5, 1, 5, 10, 50 and 100 μM . A 3 mL water sample was mixed with 0.12 ml of Phenol Solution, 0.12 ml of Sodium Nitroorusside Solution, and 0.3 mL of Oxidizing Solution in test tubes that have been pre-reacted with the reagents. The samples sat in the dark at room temperature for 1 hour and absorptions were run on the Shimadzu 1601 spectrophotometer.

Sulfate samples were diluted 400:1 and loaded on the AS40 Automated Sampler in 0.5 ml DionexTM vials. Samples were analyzed on the DionexTM DX-120 Ion Chromatograph (Staff, 2006).

A method adapted from Gilboa-Garber (1971) was used to analyze H_2S in the water samples. The zinc acetate and water mixture was mixed with 5 mL of dye solution and sat in the dark for 45 minutes. Absorbencies were read on the spectrophotometer set at 670 nm.

Iron samples were analyzed using the Perkin-Elmer 2380 atomic absorption spectrometer (AAS).

Results

Iron

Woodchips used were previously treated with iron and thoroughly washed off, however after extraction and analysis iron was found on the chips. The control microcosms will be referred to as low iron treatment and the iron microcosm will be referred to as high iron treatment. The low iron microcosm contains approximately $5.94 \text{ g Fe microcosm}^{-1}$ and the high iron microcosms contain $20.03 \text{ g Fe microcosm}^{-1}$.

Higher outflow concentrations of iron were observed in the low iron microcosm. Outflow iron concentrations in the high iron microcosms ranged from 1-10 ppm Fe and 10-40 ppm Fe in the low iron microcosms (Figure 1).

Nitrate

Nitrate concentration of the inflow water in both the low and high iron microcosms is between 120 and 180 μM . The outflow concentration of nitrate in the low iron microcosm is minimal, reaching a maximum of 8 μM on day 9. Nitrate concentrations in the outflow of the high iron microcosms are also minimal, but reach a peak near day 9 of $\sim 60 \mu\text{M}$ (Figures 2, 3).

Ammonium

Outflow water in the low and high iron microcosms show higher concentrations of ammonium than the inflow. Inflow ammonium concentrations remain around 1 μM in both microcosms (Figures 4, 5). Ammonium production is lower in the high iron treatment (Figure 6).

Hydrogen Sulfide

No detectable amount of hydrogen sulfide was found in the outflow of the control and iron microcosms.

Sulfate

No significant difference was seen between sulfate inflow and outflow concentrations. Both treatments are around 28 mM through the duration of the experiment (Figures 7, 8).

Depth Profiles

The low and high iron treated microcosms show decreasing amounts of nitrate with depth. The low iron microcosm has 40 μM nitrate at 2 cm and the high iron microcosm has a nitrate concentration of 110 μM at 2 cm. The two treatments show similar concentrations after 16 cm. Nitrate concentrations in low and high iron treatments dropped to near 1 μM at 32 cm (Figure 9).

Ammonium concentrations in the low iron microcosm remain around 1-3 μM at all depths. The high iron microcosm also shows similar concentrations except an ammonium peak reaching 13 μM seen at 16 cm (Figure 11).

Sulfate concentrations range from 26,500 to 27,000 μM in the low iron. The high iron microcosm shows a similar trend, but also has a peak at 16 cm reaching 28,000 μM sulfate (Figure 12).

No detectable amount of hydrogen sulfide was found at any depth in the microcosms.

Carbon and Nitrogen Analysis

C:N ratios for the original, low iron 8 cm, 32 cm and high iron 8 cm wood chips are around 800. The C:N ratio of high iron 32 cm woodchips was around 600 (Figure 13).

Discussion

The data indicates that the microcosms are effective at removing nitrate from the inflow. Concentrations of nitrate decrease from 150-200 μM in the inflow to a concentration of 5-10 μM in the outflow (Figures 2, 3). A spike of nitrate in the outflow of the iron microcosm reaches 60 μM and could be the result of contamination or exposure of the microcosm to oxygen. It can be concluded that the addition of iron oxide does not have an inhibitory effect on the removal of nitrate in the microcosms.

Ammonium outflow is below 7 μM in both microcosms with the exception of an outlier of 25 μM at day 9 (Figures 4, 5). Almost no ammonium production is seen by the end of experiment in the high iron treatment (Figure 6). Data obtained from previous microcosm studies show ammonium production around 12 μM (Anderson, 2006). The addition of iron to the microcosms shows a decrease in the production of ammonium.

Since high levels of hydrogen sulfide stimulate DNRA (Brunet and Garcia-Gil, 1996) and ammonium production, I proposed to eliminate H_2S by adding iron oxide, fueling the formation of FeS . No detectable amounts of hydrogen sulfide were found in the outflow of either iron treated microcosm. Previous studies found hydrogen sulfide concentrations around 100 μM in the outflow of non-iron microcosms with a seawater inflow (Andersen, 2006).

Sulfate inflow and outflow are relatively equal in both treatments (Figures 7, 8) and no detectable amount of hydrogen sulfide was found in the outflow of the microcosms. This data indicates that the addition of iron somehow inhibited sulfate reduction in the microcosms. Sulfate reduction is inhibited by Fe (III) reducers because they out-compete sulfate reducers for electron donors (Lovely, 1991). Fe (III) reducers have the capability to metabolize electron donors down to concentrations below the ability of sulfate reducers (Lovely, 1991). Roden and Wetzel (1996) also found that the Fe(III) reduction could outcompete sulfate reduction in iron rich wetlands.

The nitrate depth profiles indicate that nitrate removal is occurring at a faster rate in the low iron microcosm, however the high and low iron microcosms showed nitrate concentrations near zero by 32 cm (Figure 9). There is no plausible explanation for the effect of iron content on the rate of nitrate removal.

The ammonium and sulfate depth profiles represent concentrations similar to their outflow concentrations. However, both high iron depth profiles have

ammonium and sulfate peaks at 16 cm (Figures 11, 12). The ammonium peak at 16 cm could be the result of a large concentration of DNRA bacteria (Figure 11), however further analysis is required to determine an explanation for the peak seen at this depth. The sulfate peak at 16 cm (Figure 12) is also unexplainable and could be the result of sampling error or microcosm defect.

Carbon and nitrogen analysis produced results that indicated no significant nitrogen accumulation on the wood chips in the low iron and high iron 8 cm chips. The high iron chips at 32 cm showed a lower C:N ratio around 600 indicating nitrogen accumulation (Figure 13). Bacterial assimilation or ammonium production could explain the lower C:N ratio, but the source of this nitrogen accumulation seen at 32 cm in the high iron microcosm is unknown. C:N ratios that are similar to the original wood chips indicate little to no nitrogen accumulation and suggest that denitrification is the most likely nitrate removal pathway. Due to the non-uniform surface area of the woodchips, reliable conclusions using C:N ratios can not be made.

Conclusions

It was hypothesized that the iron addition would trap hydrogen sulfide in the microcosms by forming FeS compounds and ultimately reduce the production of ammonium. After data analysis it was determined that the addition of iron oxide actually inhibited sulfate reduction and thus the production of hydrogen sulfide. Since no hydrogen sulfide was present, the number of sulfur oxidizing bacteria capable of DNRA was minimized, along with the production of ammonium.

The iron addition appeared to have no effect on nitrate removal in lab settings, however it is unknown if the unnatural iron concentrations would have any adverse effects if applied in the environment. The addition of iron oxide also showed to reduce the ammonium production in microcosms from 12 μM to concentrations less than 5 μM .

Further analysis is needed to determine the amount of nitrate removal accounted for through denitrification. Another study is also necessary to determine how applicable an iron addition to the woodchips is in the environment and the minimal amount of iron needed to reduce ammonium production.

Acknowledgements

I would like to thank Joe Vallino and Anne Giblin for their advice and mentoring during this project. I would also like to thank Ken Foreman for his interest and help throughout my project. I am very grateful for the help of Rich McHorney in assembling and maintaining the microcosms. I would also like to extend my gratitude to TA's Beth Bernhart, Will Longo, and Ylva Olsen for analysis help, and all SES students for their help and encouragement and making the semester an enjoyable experience.

Literature Cited

- Andersen, Jesper H., Louise Schluter and Gunni Ertebjerg. 2006. Coastal eutrophication: recent developments in definitions and implications for monitoring strategies. *Journal of Plankton Research*. 28(7): 621-628.
- Anderson, Mark. 2006. Mechanisms of Nitrate Removal in Permeable Reactive Barriers. Final SES Project. Marine Biological Laboratory.
- Burgin, Amy J., Stephen K. Hamilton. 2007. Have we overemphasized the role of denitrification in aquatic ecosystems? A review of nitrate removal pathways. *Front Ecol Environ*; 5(2): 89-96.
- Brunet, R., and L. Garcia-Gil. 1996. Sulfide-induced dissimilatory nitrate reduction to ammonia in anaerobic freshwater sediments. *FEMS Microbiology Ecology* 21:131-138.
- Gilboa-Garber, N. 1971. Direct spectrophotometric determination of inorganic sulfide in biological materials and in other complex mixtures. *Analytical Biochemistry* 43: 129-133.
- Lovley, D. R. 1991. Dissimilatory Fe(III) and Mn(IV) reduction. *Microbiol. Rev.* 55: 259-287.
- Roden, Eric E. and Robert G. Wetzel. 1996. Organic carbon oxidation and suppression of methane production by microbial Fe(III) oxide reduction in vegetated and unvegetated freshwater wetland sediments. *Limnol Oceanogr.* 41(8): 1733-1748.
- Schwarzman, Beth. The Nature of Cape Cod. University Press of New England: Lebanon, 2002; pp.74-75.
- Solarzano, L. (1969). Determination of ammonium in natural waters by phenol hypochlorite method. *Limnol. Oceanogr.*, 14:799-800
- Staff, SES. 2006. Dionex-120 Manual. Laboratory Manual for Semester in Environmental Science, Marine Biological Laboratory.
- Wood, E.D., F.A.G. Armstrong, and F.A. Richards. 1967 Determination of nitrate in seawater by cadmium-copper reduction to nitrate. *J. Mar. Biol Assoc. U.K.* 47:23.
- Valiela, Ivan. Marine Ecological Processes. Springer-Verlag: New York, 1984; pp. 515-528.

Vincent, Angela. 2006. The Effects of Seawater Intrusion on Microbial Nitrate and Sulfate Reduction within a NITREX™ Permeable Reactive Barrier Designed to Mitigate Groundwater N-Pollution. Final SES Project. Marine Biological Laboratory.

Figures

Figure 1. Iron Content in Outflow of Microcosms

Figure 2. Nitrate Inflow and Outflow in the Low Iron Treatment

Figure 3. Nitrate Inflow and Outflow in the High Iron Treatment

Figure 4. Ammonium Inflow and Outflow in the Low Iron Treatment

Figure 5. Ammonium Inflow and Outflow in the High Iron Treatment

Figure 6. Ammonium Production in Microcosms

Figure 7. Sulfate Inflow and Outflow in the Low Iron Treatment

Figure 8. Sulfate Inflow and Outflow in the High Iron Treatment

Figure 9. Nitrate Depth Profile in Microcosms

Figure 10. Nitrate Depth Profile with Exponential Curve

Figure 11. Ammonium Depth Profile in Microcosms

Figure 12. Sulfate Depth Profile in Microcosms

Figure 13. C:N Ratios of Woodchips in Microcosms

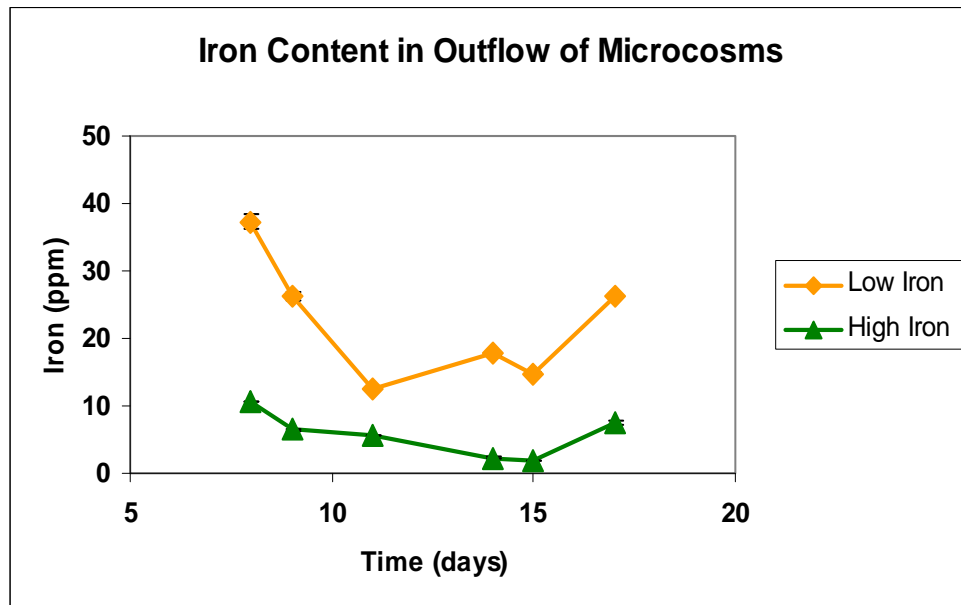


Figure 1. Iron Content in Outflow of Microcosms

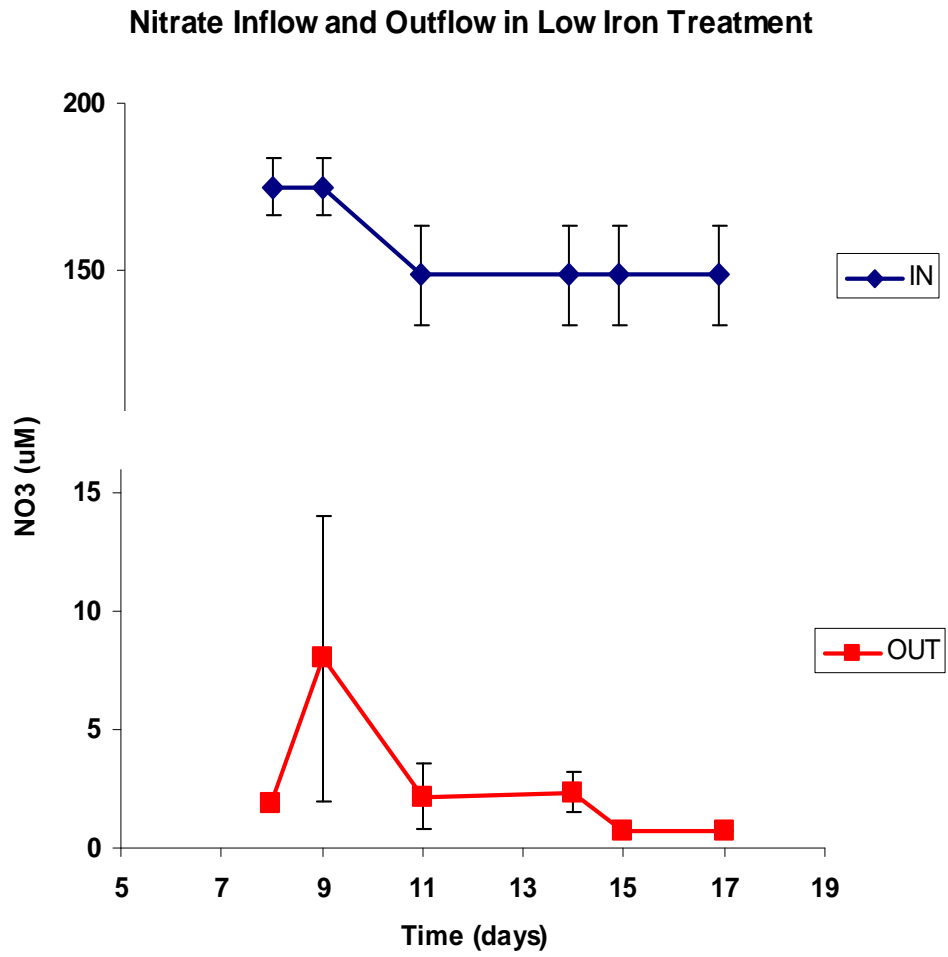


Figure 2. Nitrate Inflow and Outflow in the Low Iron Treatment

Nitrate Inflow and Outflow in High Iron Treatment

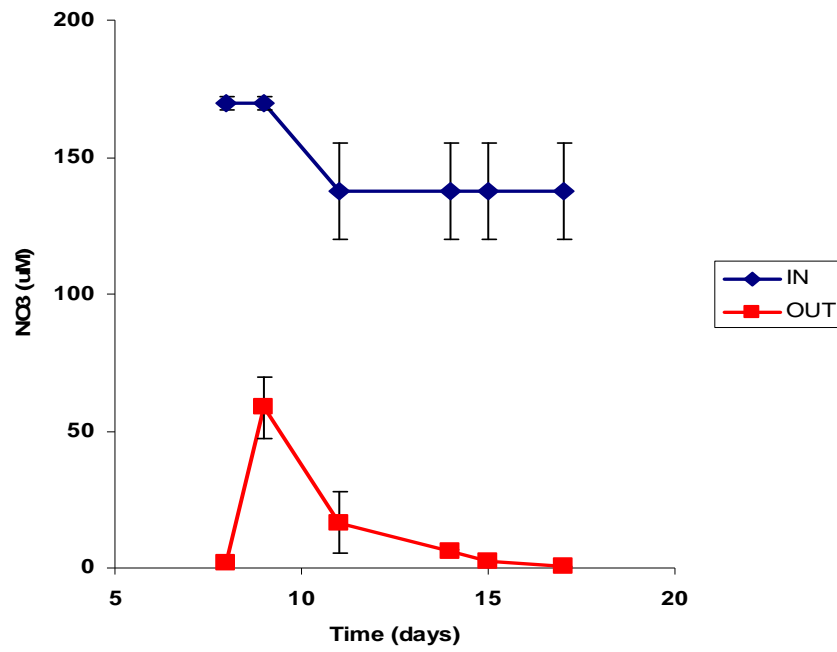


Figure 3. Nitrate Inflow and Outflow in the High Iron Treatment

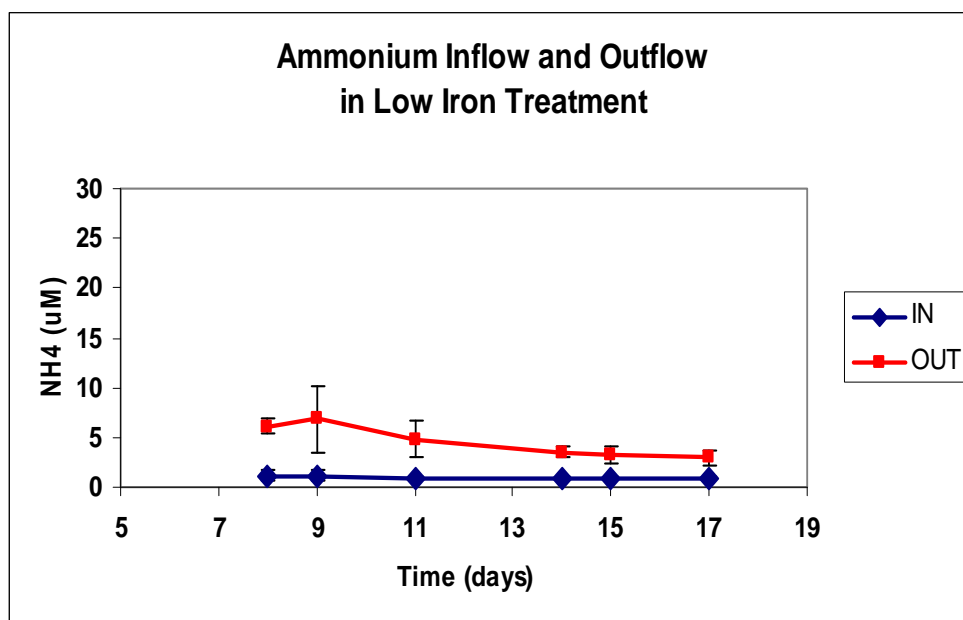


Figure 4. Ammonium Inflow and Outflow in the Low Iron Treatment

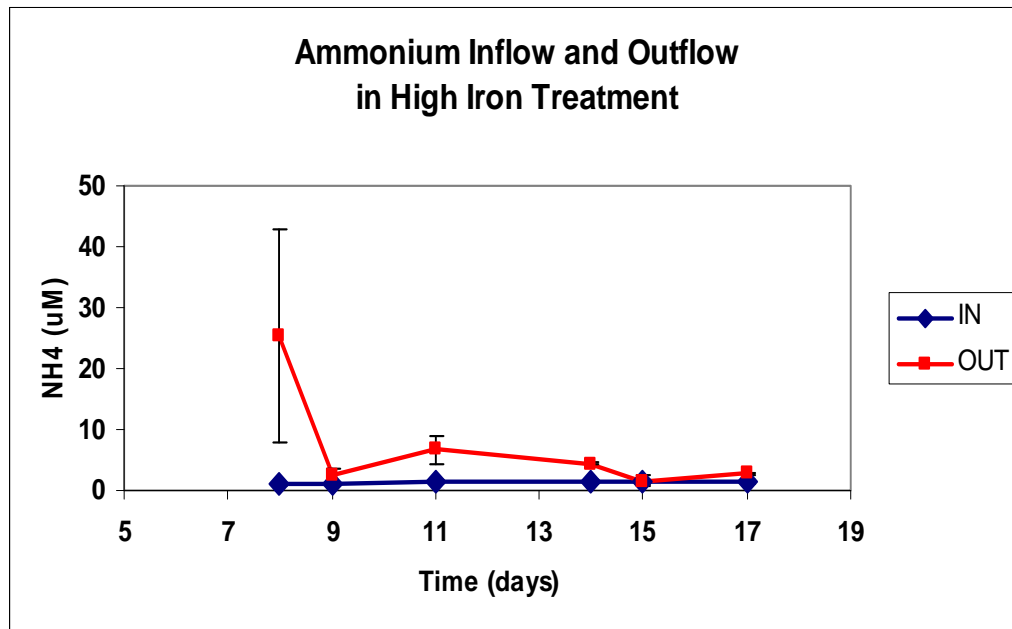


Figure 5. Ammonium Inflow and Outflow in the High Iron Treatment

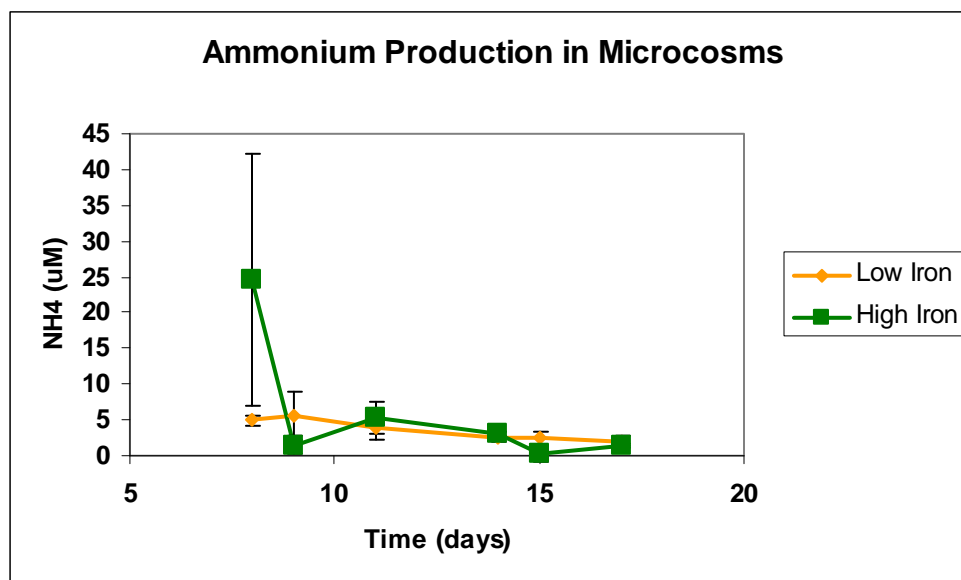


Figure 6. Ammonium Production in Microcosms

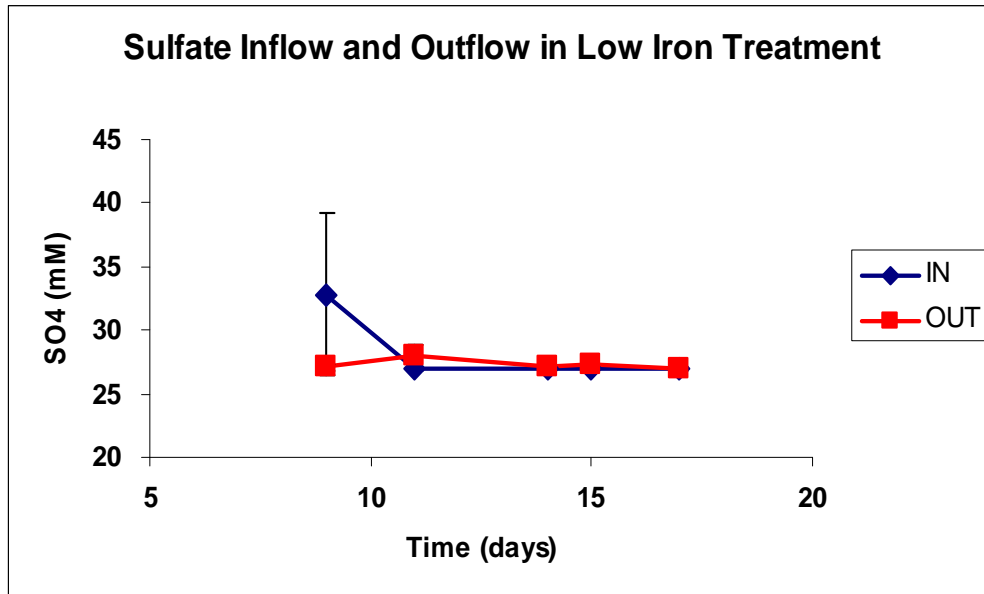


Figure 7. Sulfate Inflow and Outflow in Low Iron Treatment

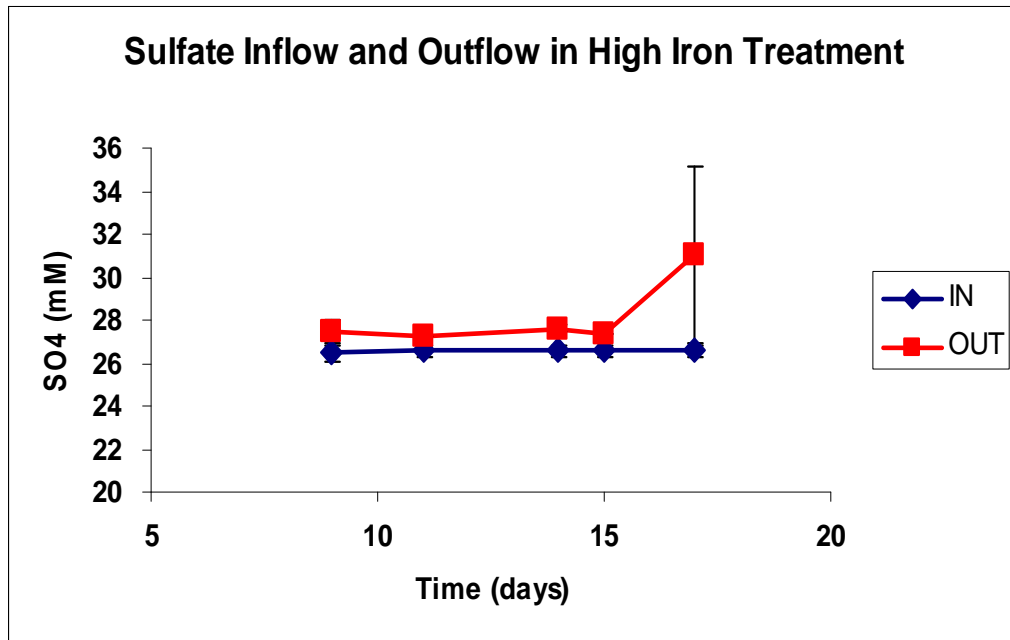


Figure 8. Sulfate Inflow and Outflow in High Iron Treatment

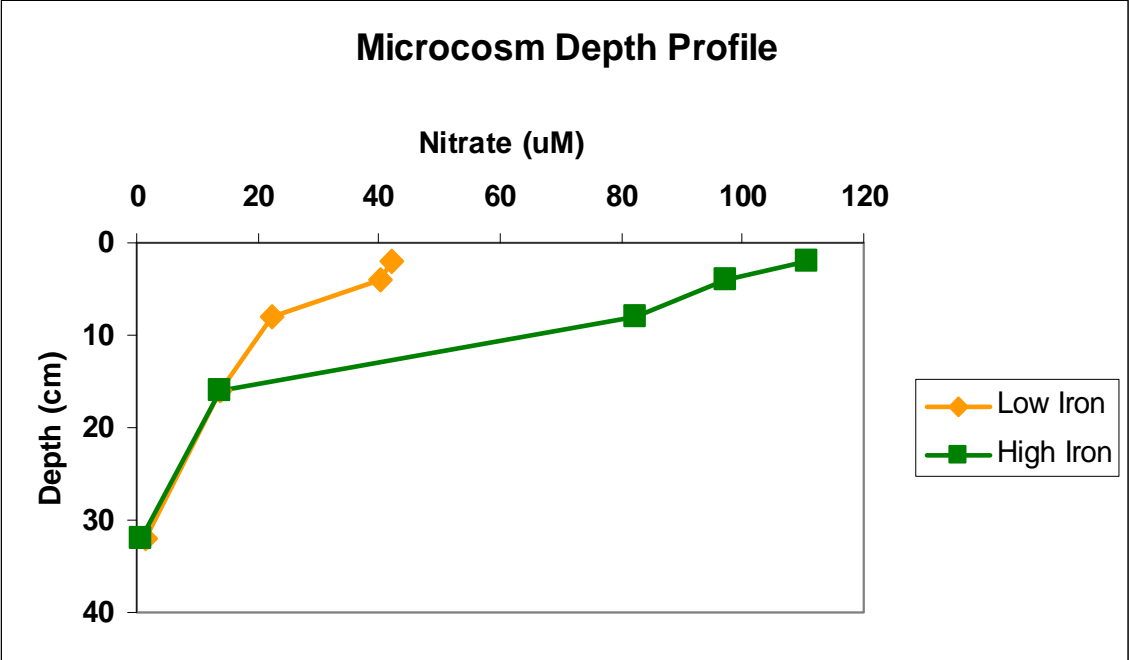


Figure 9. Nitrate Depth Profile

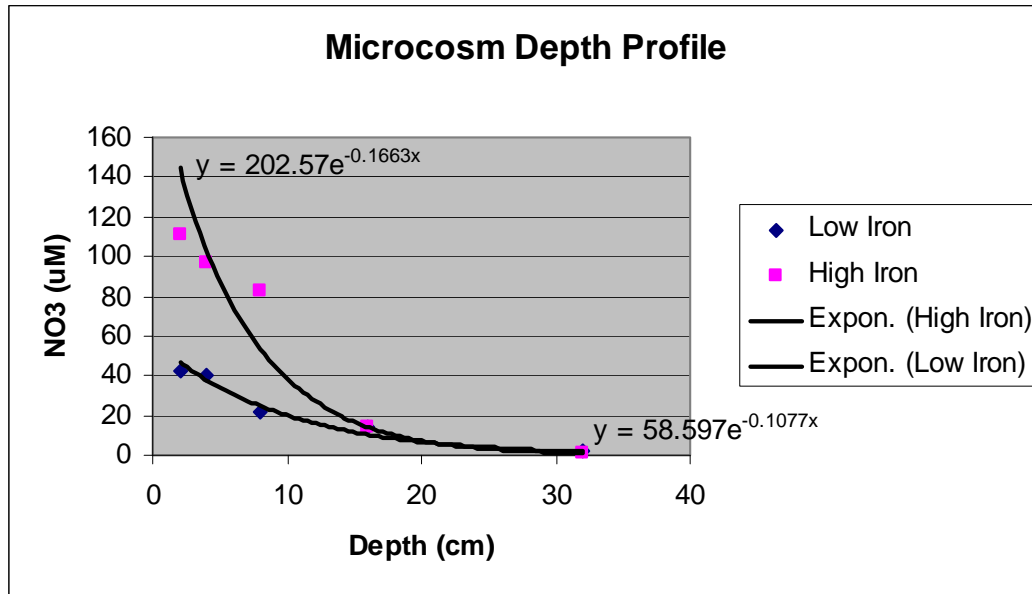


Figure 10. Nitrate Depth Profile with Exponential Curve

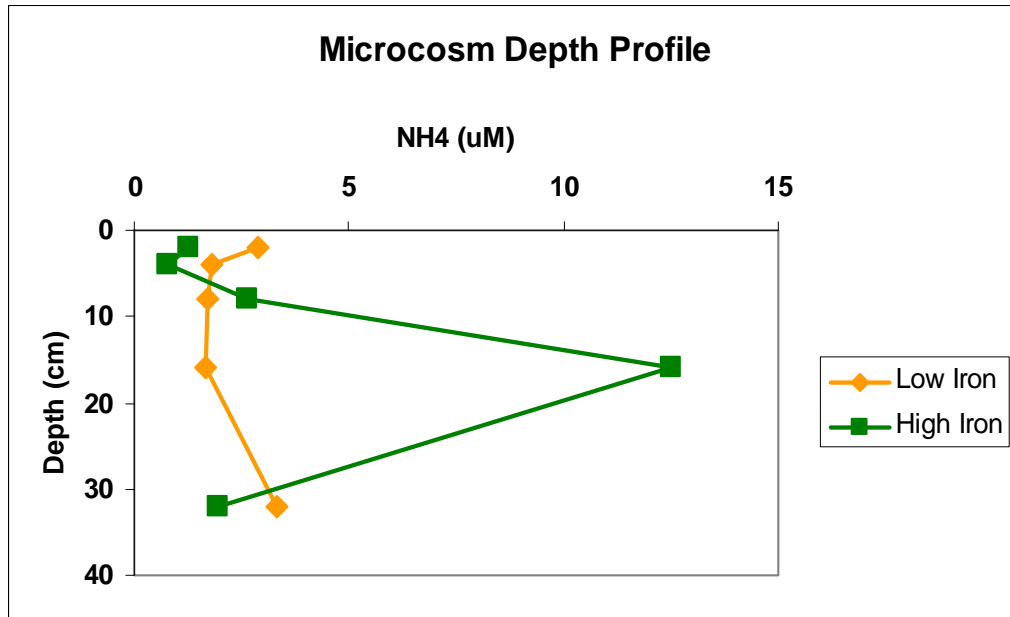


Figure 11. Ammonium Depth Profile

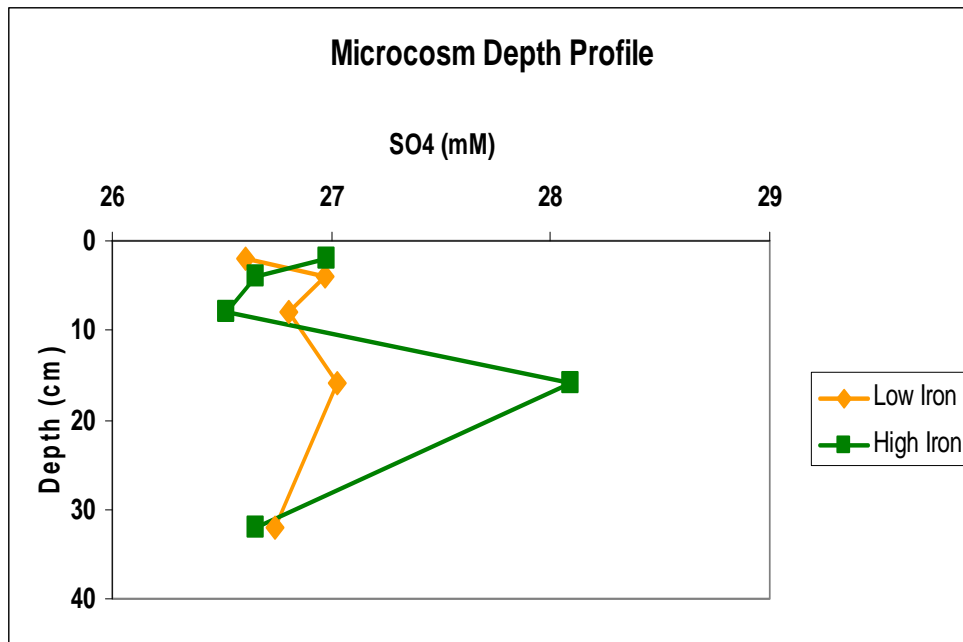


Figure 12. Sulfate Depth Profile

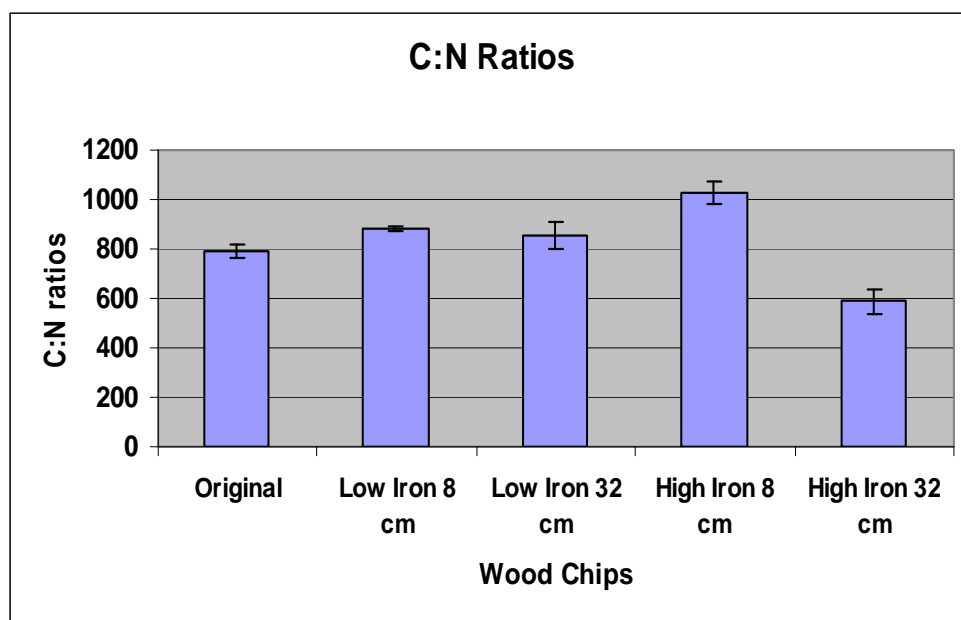


Figure 13. C:N Ratios in Woodchips in Microcosms